Utilising whey water to produce bacterial cellulose-based insulin patch

Team GEnoM[1]

Department of Biotechnology, Indian Institute of Technology Madras, Chennai, India {igem@smail.iitm.ac.in}

Abstract. Industrial whey wastewater discharge is of great environmental concern. With ever increasing production and wastage rates, we intend to utilize the whey wastestream as our feedstock to produce bacterial cellulose(BC) by engineering different strains of the *K.xylinus* species to metabolize lactose thus paving the way for the production of BC based hydrogels. The hydrogel produced will be used to manufacture patches which contain a set dose of insulin which can be painlessly and efficiently delivered to a patient in a controlled manner.

Keywords: Synthetic biology · Whey waste · *K.xylinus* · Genome-scale metabolic models · Hydrogels · Insulin patch.

1 Introduction

Every year approximately 190 million tonnes of whey is generated as wastewater effluent[2]. In addition to this, it is known that 50 percent of the total whey is recycled and converted into whey protein and its isolates, which undoubtedly drives today's health market. The other half is discharged unsupervised, just like several other industrial effluents in the world. This is a major cause of concern as whey has an incredibly high organic load due to the presence of an organic sugar lactose. This affects the BOD of water bodies depleting aquatic oxygen levels[6]. On the other hand, diabetes is a major health risk in India, owing to the 128 % increase of diabetic patients from 1990 to 2013. Insulin is a peptide hormone that is used in the treatment of diabetes. Syringes and insulin pens are the standard ways of delivery of insulin therapy. These methods have many disadvantages such as the disposal of needles, non-biodegradability, and more importantly, it's invasiveness. Insulin pills are slow-acting and have a lot of side effects such as weight gain, anxiety etc. Other techniques such as insulin pumps and infusers may cause skin infections and are expensive. These intensive and invasive techniques motivate the need for an alternative more user-friendly, effective and reliable method of drug delivery. The use of chemical penetration enhancers (CPEs) is an attractive alternative in terms of economic viability and ease of applicability[20]. Our Project aims at developing a solution that addresses both these issues. Bacterial nanocellulose (BNC) is a pure form of cellulose synthesized by acetic acid bacteria such as *Gluconacetobacter xylinus*, *Gluconacetobacter hansenii*, *Komagataeibacter xylinus*, etc which has several properties such as biocompatibility, high mechanical strength, biodegradability, nil toxicity, high crystallinity, chemical and morphological controllability that makes it suitable for drug delivery. The main advantages of using BNC biomembranes for insulin delivery are the possibility of controlled drug release over time and also painless administration through insulin patches.

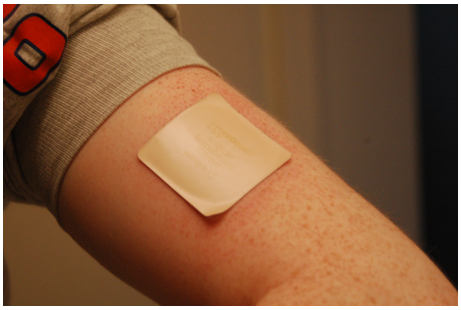

Fig. 1: Smart adhesive insulin patch

2 Methods and Results

2.1 Building a genome-scale metabolic model

Introduction

Whey contains about 95 % water, some amount of proteins and the remaining is lactose. The main carbon content of the whey is 75% anhydrous lactose[2]. Bacterial cellulose producing acetic acid bacteria such as *Gluconacetobacter hansenii*, *Komagataeibacter xylinus* do not have the enzymes to break down lactose and metabolise it. Therefore, we propose to genetically modify *Komagataeibacter xylinus* to efficiently utilise lactose by the following steps:
* Engineering *K. xylinus* gal(-) strain with lacZ gene
* Engineering *K.xylinus* gal(+) strain with uridyltransferase and galactokinase to metabolise galactose
* Co-culturing both the mutant bacterial strains in whey

The experimental introduction of these genes are designed using the toolbox built by the iGEM Imperial team 2014. Our backbone vector is pSEVA331Bb, and each of the genes are flanked by BBa_J2310 Promoter, B0034 Strong RBS, B0015 Double terminator and restriction enzymes sites for introduction into pSEVA.

Evidence for choosing the above enzymes comes by effectively analysing the lactose and galactose metabolism in *Komagataeibacter xylinus* strain, as given in the pathway in Figure 2. We modelled this using COBRA toolbox of MATLAB by building genome scale metabolic models of two strains of bacteria to better judge how they would metabolise whey. We plan to use this as our basis to guide our future wetlab experiments to introduce the respective genes into the 2 strains.

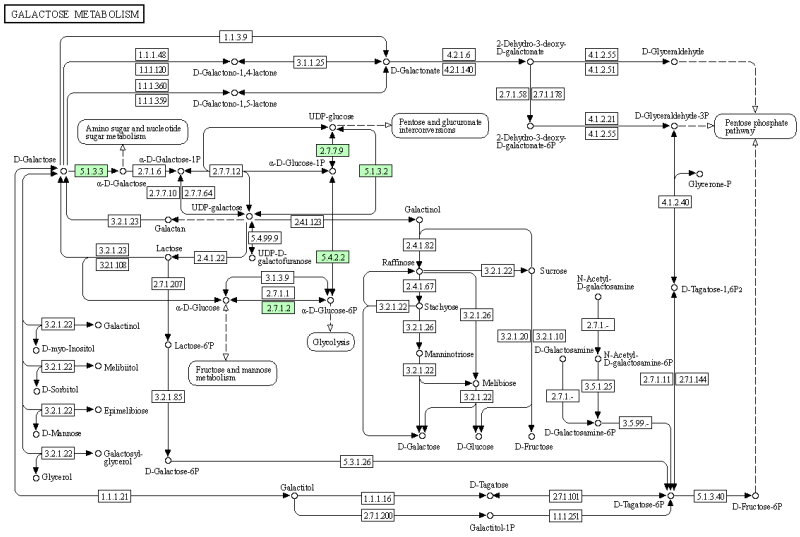

Fig. 2: Lactose and Galactose metabolism pathway of *K.xylinus*. The ones in green are the enzymes present in the strain.

Genome-scale metabolic models represent an organism's metabolic network and incorporate Gene-Protein-reaction (GPR) rules to represent the relationship between the genes encoding enzymes and the various metabolic reactions they catalyze. Flux balance analysis on such models has been used to predict phenotypes of various organisms under different environmental conditions.
A Genome scale metabolic model was built from the *K.xylinus* E_25 strain genome using K_base. We created two strains using COBRA toolbox by introducing relevant constraints. Strain 1 was the original model as it already had the B-gal gene that is responsible for the enzyme that metabolizes lactose. Strain 2 was created by adding two extra reactions for metabolising galactose.
Formation of Gal1P from Galactose:

$$atp\_c + a\_gal\_\_D\_c \rightleftharpoons adp\_c + gal1p\_c + h\_c \tag{2.1}$$

Conversion of Gal1P to UDP- Galactose:

$$gal1p\_c + h\_c + utp\_c \rightleftharpoons ppi\_c + udpgal\_c \tag{2.2}$$

Cellulose production did not have an explicit reaction in the model. Thus, to measure the flux of bacterial cellulose production, we introduced three additional reactions to the model- cellulose production from UDP glucose, cellulose exchange between the cytoplasm and the extracellular region, and a sink reaction for extracellular cellulose.
Formation of Cellulose from UDP- Glucose:

$$udpg\_c \rightleftharpoons udp\_c + Cellulose\_c \tag{2.3}$$

Cellulose Exchange:

$$Cellulose[c0] \rightarrow Cellulose[e0] \tag{2.4}$$

Cellulose Sink:

$$Cellulose[e0] \rightarrow \tag{2.5}$$

Strain 1 was constrained to take up lactose as the sole carbon source from the medium, while Strain 2 was constrained similarly on galactose. The maximum possible cellulose fluxes were obtained by setting cellulose production as the objective function. Biomass flux decreases with increase in cellulose flux as seen in Fig 3.

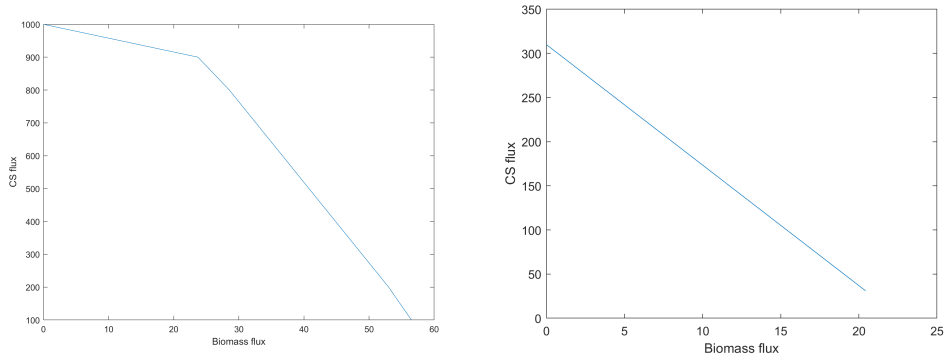

(a) (b)

Fig. 3: Cellulose flux versus biomass flux for **a.**Strain 1 **b.**Strain 2.

Constraining strain 1 to produce an optimal 400 mmol gDW^{-1} hr^{-1} keeps biomass at around 44.85 mmol gDW^{-1} hr^{-1}, which is not a great decrease from the maximum biomass flux of 60 mmol gDW^{-1} hr^{-1}. Similarly, constraining strain 2 to produce 50 mmol gDW^{-1} hr^{-1} keeps biomass at around 19 mmol gDW^{-1} hr^{-1}.

2.2 FSEOF

The method used for selecting genes for overexpression of cellulose is FSEOF (Flux Scanning based on Enforced Objective Flux). Cellulose production is like the production of secondary metabolites (not growth-coupled). Hence, other methods like OptKnock, that use coupled growth and product flux are not very useful. Gene deletions are usually more harmful to the system than gene overexpression. FSEOF, hence, provides the advantage of predicting overexpression targets, without a necessary growth-coupling. For FSEOF, the theoretical maximum cellulose flux is first obtained by setting the objective function to cellulose production. As the flux through the cellulose reaction is increased step by step upto the theoretical maximum, FBA is applied to maximize biomass at each step, and the reactions that show increased flux with this increasing cellulose flux are potential targets. This is seen in Figure 4a. The overexpression target reactions found by applying this principle to each strain individually are found in Figure 4b.

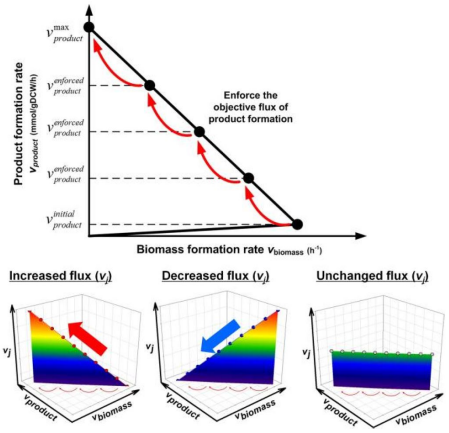

(a)

Strain 1	UTP:alpha-D-glucose-1 -phosphate uridylyltransferase_c0	alpha-D-Glucose 1-phosphate 1,6-phosphomutase_c0	All Cellulose reactions added	
Strain 2	D-glucose-6-phosphate aldose-ketose-isomeras e_c0	ATP:UDP phosphotransferase_c0	2-Phospho-D-glycerate 2,3-phosphomutase_c0	All Cellulose reactions added

(b)

Fig. 4: **a.**FSEOF methodology. Those reactions that show an increased flux with increasing product flux are selected for overexpression (Choi et al., 2010). **b.**Selected reactions for overexpression

2.3 Co-culturing two *K.xylinus* strains for Lactose and Galactose metabolism

To further characterize the behaviour when both the strains are grown together, we attempted to build a Multi-species model on Cobra Toolbox. We used the inbuilt 'createMultispeciesmodel' function and 'SteadyCom' to run the generated joint model. Unfortunately we were unable to completely verify the growth of the combined model due to time constraints and some minor errors. During this trial, the system constraints determined the combined survival of both the models in the co-culture. In the absence of proper constraints, growth was observed in only one model. Further work will be continued on this.

2.4 Modelling the effectiveness of insulin patch made out of bacterial cellulose

Introduction

The bacterial cellulose produced by our strain can be used to produce hydrogels for insulin patches. This modeling section describes our attempt in analysing the potential of bacterial cellulose for such an application. Our primary objective is to model the effectiveness of the insulin patch made out of bacterial nanocellulose. To understand that, we break down the modeling into two steps.
Step 1: Modelling the adsorption of insulin in the Bacterial Nanocellulose (BNC)
Step 2: Modelling the release rate of the insulin through the skin from the BNC patch
We also aim to understand the role of Chemical penetration enhancers in altering the permeability of insulin through the skin.

2.5 Adsorption of insulin in Bacterial nanocellulose (BNC)

BNC biomembranes are widely studied for their controlled drug delivery. Several studies[4] such as Fourier transform infrared (FTIR) analyses of BNC membrane with adsorbed insulin suggest that the chemical aspect of insulin is preserved during the integration into BNC biomembrane suggesting that insulin is getting adsorbed and not absorbed. Thermal analysis[4] of BNC with insulin suggests that the incorporation of insulin did not compromise the stability of the BNC biomembrane ensuring a greater shelf life[15]. For insulin adsorption assays, the biomembrane produced by the acetic acid bacterium is washed in NaOH and then soaked in a buffered solution of Human insulin. We can consider that the amount of insulin sorbed is a very small fraction of total insulin present in the solution. Thus insulin concentration far from the surface of BNC does not change[15]. The adsorption process follows unsteady-state diffusion.

Using equations of continuity in rectangular coordinate system[16],

$$\frac{\partial c_i}{\partial t} + \vec{V}.\vec{\nabla}\vec{c_i} - D_i(\frac{\partial^2 c_i}{\partial x^2} + \frac{\partial^2 c_i}{\partial y^2} + \frac{\partial^2 c_i}{\partial z^2}) = R_i$$

Since there is no convection, we can ignore second term. Since $c_i \neq f(x)$ and $c_i \neq f(y)$ and there is no reaction

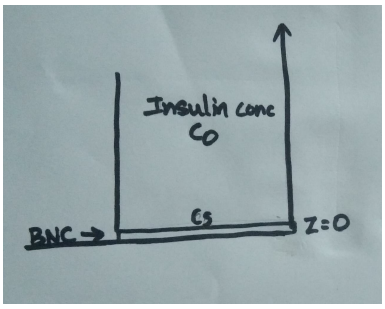

Fig. 5: Adsorption of Insulin by BNC: at z=0, the BNC biomembrane is placed and the concentration of the surface of BNC is c_s while the concentration of the solution is c_o

as well, the equation gets reduced to,

$$\frac{\partial c_i}{\partial t} - D_i \frac{\partial^2 c_i}{\partial z^2} = 0 \tag{2.6}$$

The initial and the boundary conditions:

$$t = 0; z \geq 0; c_i = c_o$$

$$t \geq 0; z = 0; c_i = c_s$$

$$t \geq 0; z \to \infty; c_i = c_o$$

In order to convert the above partial differential equation(PDE) to ordinary differential equation(ODE), we define the following dimensionless variables:

$$\theta = \frac{c_i - c_o}{c_s - c_o}$$

$$\eta = \frac{z}{\sqrt{4D_i t}}$$

Here, $\theta = f(\eta)$ and $\eta = f(z,t)$. Using chain rule we aim to find $\frac{\partial c_i}{\partial t}$and $\frac{\partial^2 c_i}{\partial z^2}$ in terms of $\frac{\partial \theta}{\partial \eta}$,$\frac{\partial^2 \theta}{\partial \eta^2}$ and $\frac{\partial \eta}{\partial z}$

$$\frac{\partial c_i}{\partial t} = (c_s - c_o)\frac{\partial \theta}{\partial \eta}(\frac{-\eta}{2t})$$

$$\frac{\partial \eta}{\partial z} = \frac{1}{\sqrt{4D_i t}}$$

This is independent of z so we can write,

$$\frac{\partial^2 c_i}{\partial z^2} = \frac{c_s - c_o}{4D_i t}\frac{\partial^2 \theta}{\partial \eta^2}$$

Substituting the above equations and simplifying, the equation reduces to

$$-2\eta \frac{d\theta}{d\eta} = \frac{d^2\theta}{d\eta^2}$$

Boundary conditions get transformed to:

$$\eta = 0; \theta = 1$$

$$\eta \to \infty; \theta = 0$$

Now this ODE can be solved by using the following substitution,

$$u = \frac{d\theta}{d\eta}$$

$$-2\eta.u = \frac{du}{d\eta}$$

This can be solved by integrating and we get the following equation,

$$\ln(u) = -\eta^2 + A$$

$$u = d\theta/d\eta = c.\exp(-\eta^2)$$

Using Leibnitz rule and solving for θ , we get

$$\theta = 1 - erf(\eta)$$

$$\frac{c_i - c_o}{c_s - c_o} = erfc(\frac{z}{\sqrt{4D_i t}})$$

Mass flux,

$$\vec{J_i} = -D_i \frac{\partial c_i}{\partial z}\bigg|_{z=0} = -D_i(c_s - c_o)\frac{\partial \theta}{\partial z}\bigg|_{z=0}$$

$$\vec{J_i} = -D_i(c_s - c_o)\frac{\partial c_i}{\partial \eta}\frac{\partial \eta}{\partial z}\bigg|_{z=0} = -D_i\frac{(c_s - c_o)}{\sqrt{4D_i t}}\frac{d\theta}{d\eta}\bigg|_{\eta=0}$$

using Leibnitz rule at $\eta = 0$,

$$\frac{\theta}{d\eta} = \frac{-2}{\sqrt{\pi}}.e^{-\eta^2}$$

$$at \eta = 0 \rightarrow \frac{\theta}{d\eta} = \frac{-2}{\sqrt{\pi}}$$

Thus the flux is,

$$\boxed{\vec{J_i} = \sqrt{\frac{D_i}{\pi t}}(c_s - c_o)} \tag{2.7}$$

Adsorption rate = flux. area

$$\boxed{\text{Adsorption rate} = \sqrt{\frac{D_i}{\pi t}}(c_s - c_o).area} \tag{2.8}$$

2.6 Transdermal diffusion of insulin in the presence of Chemical penetration enhancers (CPEs)

Chemical penetration enhancers are those substances that increase the permeability of the skin by interacting with its outermost layer stratum corneum which is the major barrier for hydrophilic macromolecules such as insulin. Several CPEs have been investigated for transdermal delivery of insulin and among those according to Abdul Ahad.et.al[12] mixtures of oleic acid, 1,8 cineole, and sodium deoxycholate in 3:7 ratio of ethanol: propylene glycol contributed to 45% improvement in insulin permeation in the presence of iontophoresis. In the study conducted by Rastogi and Singh[15], the K_p value of skin in the presence and absence of oleic acid as CPE is 0.0038 and 0.0007 respectively. The algorithmic study on QSPR models of several CPEs conducted by K.M. Yerramsetty et. al[12] suggested that greater hydrophobicity and reactivity increase a CPEs efficacy, and higher dipole moments decrease the efficacy. Let us incorporate oleic acid(CPE) on the adsorbed insulin patch made out of Bacterial nanocellulose. To understand the amount of drug that is absorbed by the skin, we shall assume that insulin diffuses through the skin by a dissolve mechanism following a steady-state process.

Since the majority of the resistance to insulin is offered by the stratum corneum layer, we believe that employing full thickness of the skin for permeation studies will lead to no disadvantage.

Using equations of continuity in cylindrical coordinate system[16],

$$\frac{\partial c_i}{\partial t} + \vec{V}.\vec{\nabla}\vec{c_i} - D_i(\frac{1}{r}\frac{\partial}{\partial r}r\frac{\partial c_i}{\partial r} + \frac{1}{r^2}\frac{\partial^2 c_i}{\partial \theta^2} + \frac{\partial^2 c_i}{\partial z^2}) = R_i$$

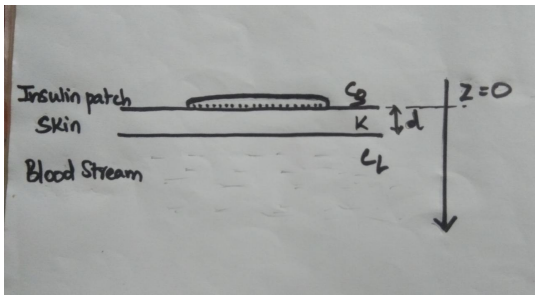

Fig. 6: Transdermal diffusion of Insulin by BNC insulin patch: at z=0 the insulin patch is placed where the concentration of insulin in c_s and the concentration of insulin below the stratum corneum is c_L, the partition coefficient is k

Since the process is in steady state and there is no convection, we can ignore the first and second term. Since $c_i \neq f(\theta)$ and $c_i \neq f(r)$ and there is no reaction as well, the equation gets reduced to,

$$D_i(\frac{\partial^2 c_i}{\partial z^2}) = 0 \tag{2.9}$$

On solving we get,

$$c_i = Az + B$$

Boundary conditions:

$$z = 0; c_i = kc_s$$
$$z = d; c_i = kc_L$$

where c_s is the concentration of insulin in the patch and c_L is the concentration of insulin in the blood stream. Using the boundary conditions and solving (2.9), we get

$$\boxed{c_i = kc_s - k(c_s - c_L)z/d} \tag{2.10}$$

Mass flux,

$$\vec{J_i} = -D_i(\frac{\partial c_L}{\partial z}) = kc_s D_i/d$$

Release rate = flux. area

$$\text{Release rate} = \frac{kc_s.D_i}{d}.area$$

Permeability of the skin can be written as

$$P = kD_i/d$$

$$\boxed{\text{Amount of drug permeated } = c_s P.t.A} \tag{2.11}$$

3 Discussion

We observe that our strains from the draft reconstruction of *K.xylinus* are able to utilize lactose and galactose, and produce bacterial cellulose. With respect to our results using FSEOF, as expected, all the cellulose reactions, synthesis and exchange are targets for overexpression of BC in both strain 1 and strain 2. We also observe that the rest of the reactions are involved in the carbon metabolism feeding into formation of the precursor of BC-UDP_glucose.

From the first model, for a BNC biomembrane of average diameter 35mm and an average weight of (75.40 $\pm$ 17.23)g[15] with an average value of diffusion coefficient of insulin in bacterial nanocellulose[14] being $7.767 * 10^{-7} cm^2/s$ and using Human insulin (Novolin ^{R} 100UI mL^{-1}; $3.5 mg_{insulin}/g_{BNC} mL^{-1}$) we can plot a graph between the amount of insulin adsorbed per unit quantity of BNC with time. Here we can observe

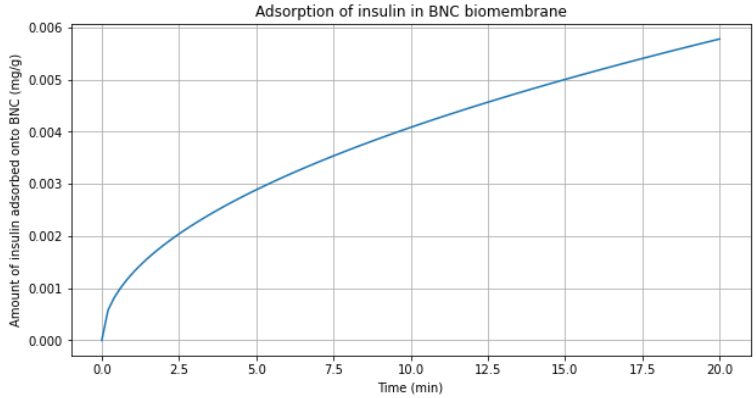

Fig. 7: Transdermal diffusion of Insulin by BNC insulin patch

that about $(6 \pm 1)\mu g_{insulin}/g_{BNC}$ is adsorbed in about 20min.

From the second model, for an insulin patch of diameter 35mm, adsorbed Human insulin (Novolin ^{R} 100UI mL^{-1}; $3.5 mg_{insulin}/g_{BNC} mL^{-1}$), diffusive coefficient of insulin in the stratum corneum of $3.97 * 10^{-12} cm^2/s$ and for a thickness of 30 μm(stratum corneum layer), we can plot the amount of insulin permeated with time both in the presence and absence of CPE(oleic acid) Here we can observe the amount of insulin permeated for different values of partition coefficient. In the presence of CPE, the k value is 0.0038 whose corresponding graph is represented in the orange line while in the absence of CPE the k value is 0.0007 which is represented by the blue graph.

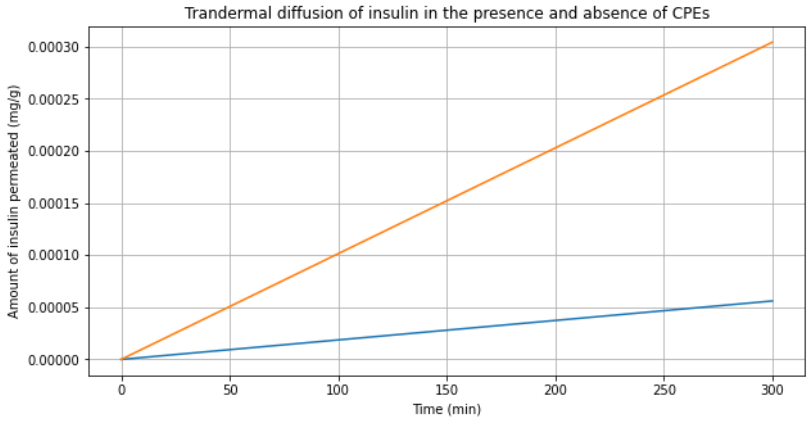

Fig. 8: Transdermal diffusion of Insulin by BNC insulin patch : orange line- k=0.0038 (with CPE); blue line- k=0.007(without CPE)

4 Conclusion

Genome scale metabolic modeling provides a simple and efficient way of analysing metabolic engineering strategies before implementing them experimentally. The developed draft reconstruction for the 2 strains represents the same. This can be used to direct future experimental work and aid the successful engineering of *K.xylinus* to produce bacterial cellulose.
Chronic diseases such as diabetes are very common and regular shots of insulin are required for those people[11]. Transdermal drug delivery provides exciting possibilities such as painless and infection-less insulin delivery. Also, the bacterial nanocellulose being biodegradable, skin sensitive, and with excellent mechanical and physicochemical properties suits the best for an insulin patch.
We mathematically analyzed the adsorption of insulin in the BNC membrane as well as the permeability analysis of insulin through the skin in the presence of chemical penetration enhancers. We also plotted the time taken for the insulin to be absorbed by the skin and the quantity of insulin absorbed which also paves way for the controlled drug release over time. Therefore bacterial cellulose is suitable for incorporating insulin, aiming at transdermal delivery.

5 Supplementary material

All our models and codes can be found in the following drive link.

Abbreviations: $\mathrm{atp}_c = AdenosineTriPhosphate(cytoplasm)$
$adp_c = AdenosineDiPhosphate(cytoplasm)$
$gal_{Dc} = DGalactose(cytoplasm)$
$gal1p_c = Galactose - 1 - Phosphate(cytoplasm)$
$h_c = HydrogenCation(cytoplasm)$
$udpgal_c = UridylylDiPhosphate - Galactose(cytoplasm)$
$ppi_c = InorganicPhosphate(cytoplasm)$
$udp_c = UridylylDiPhosphate(cellulose)$
$udpg_c = UridylylDiPhosphate - Glucose(cytoplasm)$
$utp_c = UridylylTriPhosphate(Cytoplasm)$

6 Biosafety

K.xylinus is a biosafety level 1 organism, and is considered a minimal potential hazard. The organism is currently used in the food industry for production of substances like nata de coco. Hence, the risks involved in working with it are low. The team will be working in a BSL-1 laboratory. We will not be working with risk group 3 or risk group 4 organisms. We will not release our genetically modified organisms or its products outside of the lab. Proper disposal of biological material will be observed. For the development of insulin patches, strict sterile conditions will have to be maintained since drug delivery is involved. The Recombinant DNA Safety Guidelines and Regulations issued by the Department of Biotechnology, Government of India in 1983 and amended in 1990 will be followed. The intended insulin patch will not be tested on humans.

References

1. Victor Revin, Elena Liyaskina, Maria Nazarkina, Alena Bogatyreva, Mikhail Shchankin,Cost-effective production of bacterial cellulose using acidic food industry by-products,Brazilian Journal of Microbiology, https://doi.org/10.1016/j.bjm.2017.12.012
2. Kolesovs, S., Semjonovs, P. Production of bacterial cellulose from whey—current state and prospects. Appl Microbiol Biotechnol 104, 7723–7730 (2020). https://doi.org/10.1007/s00253-020-10803-9
3. Evelyn Battad-Bernardo, Sharon L McCrindle, Iain Couperwhite, Brett A Neilan, Insertion of an E. coli lacZ gene in Acetobacter xylinus for the production of cellulose in whey, FEMS Microbiology Letters, Volume 231, Issue 2, February 2004, Pages 253–260, https://doi.org/10.1016/S0378-1097(04)00007-2

4. Hall PE, Anderson SM, Johnston DM, Cannon RE. Transformation of Acetobacter xylinum with plasmid DNA by electroporation. Plasmid. 1992 Nov;28(3):194-200. https://doi.org/10.1016/0147-619X(92)90051-b
5. Jang, Woo Dae, et al. "Genomic and Metabolic Analysis of Komagataeibacter Xylinus DSM 2325 Producing Bacterial Cellulose Nanofiber." Biotechnology and Bioengineering, vol. 116, no. 12, 2019, pp. 3372–81. Wiley Online Library, https://doi.org/10.1002/bit.27150.
6. Panghal, Anil, et al. "Utilization of Dairy Industry Waste-Whey in Formulation of Papaya RTS Beverage." Current Research in Nutrition and Food Science Journal, vol. 5, no. 2, Aug. 2017, pp. 168–74.
7. "Cost-Effective Production of Bacterial Cellulose Using Acidic Food Industry by-Products." Brazilian Journal of Microbiology, vol. 49, Nov. 2018, pp. 151–59. www.sciencedirect.com, https://doi.org/10.1016/j.bjm.2017.12.012.
8. Huang, Long-Hui, et al. "Tailoring Bacterial Cellulose Structure through CRISPR Interference-Mediated Down-regulation of GalU in Komagataeibacter Xylinus CGMCC 2955." Biotechnology and Bioengineering, vol. 117, no. 7, 2020, pp. 2165–76. Wiley Online Library, https://doi.org/10.1002/bit.27351.
9. Singh, Amritpal, et al. "Engineering Bacterial Cellulose by Synthetic Biology." International Journal of Molecular Sciences, vol. 21, no. 23, Jan. 2020, p. 9185. www.mdpi.com, https://doi.org/10.3390/ijms21239185.
10. Teh, Min Yan, et al. "An Expanded Synthetic Biology Toolkit for Gene Expression Control in Acetobacteraceae." ACS Synthetic Biology, vol. 8, no. 4, Apr. 2019, pp. 708–23. ACS Publications, https://doi.org/10.1021/acssynbio.8b00168.
11. Mohite, Bhavana V., et al. "Bacterial Cellulose-Based Hydrogels: Synthesis, Properties, and Applications." Cellulose-Based Superabsorbent Hydrogels, Springer International Publishing, 2019, pp. 1255–76. Springer Link, https://doi.org/10.1007/978-3-319-77830-32.
12. Yerramsetty KM, Neely BJ, Madihally SV, Gasem KA. A skin permeability model of insulin in the presence of chemical penetration enhancer. Int J Pharm. 2010;388(1-2):13-23. doi:10.1016/j.ijpharm.2009.12.028
13. Ahad, A.; Raish, M.; BinJardan, Y.A.; Al-Mohizea, A.M.;Al-Jenoobi, F.I. Delivery of Insulin via Skin Route for the Management of Diabetes Mellitus: Approaches for Breaching the Obstacles. Pharmaceutics 2021, 13, 100. https://doi.org/10.3390/pharmaceutics 13010100
14. Al Hanbali, O. A., Khan, H. M. S., Sarfraz, M., Arafat, M., Ijaz, S., Hameed, A. (2019). Transdermal patches: Design and current approaches to painless drug delivery. Acta Pharmaceutica, 69(2), 197–215. doi:10.2478/acph-2019-0016
15. Ludmilla R. Jorge, Liliam K. Harada and Erica C. Silva et al. BACTERIAL NANOCELLULOSE BIOMEMBRANE AS A SUPPORT FOR HUMAN INSULIN AIMING AT TRANSDERMAL PERMEATION. Quím. Nova. Vol. 43(5):572-578. DOI: 10.21577/0100-4042.20170522
16. G.K. Suraishkumar. Continuum Analysis of Biological Systems. Springer-Verlag Berlin Hei-delberg, 2014.
17. Leeladurga, V., Teja, U.C., Sultana, S.K.A. et al. Application of Microneedle Arrays for Enhancement of Transdermal Permeation of Insulin: In Vitro Experiments, Scaling Analyses and Numerical Simulations. AAPS PharmSciTech 17, 915–922 (2016). https://doi.org/10.1208/s12249-015-0416-8
18. https://ecommons.cornell.edu/bitstream/handle/1813/43906/Group07.pdf? sequence=2
19. https://www.medicalnewstoday.com/articles/around-5-percent-of- people-may-achieve-remission-from-type-2-diabetesFuture-prevention
20. Rastogi SK, Singh J. Effect of chemical penetration enhancer and iontophoresis on the in vitro percutaneous absorption enhancement of insulin through porcine epidermis. Pharm Dev Technol. 2005;10:97–104.
21. Jang, Woo Dae, et al. "Genomic and Metabolic Analysis of Komagataeibacter Xylinus DSM 2325 Producing Bacterial Cellulose Nanofiber." Biotechnology and Bioengineering, vol. 116, no. 12, 2019, pp. 3372–81. Wiley Online Library, https://doi.org/10.1002/bit.27150.
22. Choi, H. S., Lee, S. Y., Kim, T. Y., Woo, H. M. (2010). In Silico Identification of Gene Amplification Targets for Improvement of Lycopene Production. Applied and Environmental Microbiology, 76(10), 3097–3105. https://doi.org/10.1128/AEM.00115-10
23. Monk, J., Nogales, J., Palsson, B. O. (2014). Optimizing genome-scale network reconstructions. Nature Biotechnology, 32(5), 447–452. https://doi.org/10.1038/nbt.2870
24. Orth, J. D., Thiele, I., Palsson, B. Ø. (2010). What is flux balance analysis? Nature Biotechnology, 28(3), 245–248. https://doi.org/10.1038/nbt.1614